Research Article

Journal of PeptideScience

Received: 27 June 2008 Revised: 22 July 2008 Accepted: 30 July 2008 Published online in Wiley Interscience: 4 November 2008

(www.interscience.com) DOI 10.1002/psc.1070

The interaction of cell-penetrating peptides with lipid model systems and subsequent lipid reorganization: thermodynamic and structural characterization‡

Isabel D. Alves,[a,b]* Isabelle Correia,[a,b] Chen Yu Jiao,[a,b] Emmanuelle Sachon,[a,b,c] Sandrine Sagan,[a,b] Solange Lavielle,[a,b] Gordon Tollin[d] and Gérard Chassaing[a,b]

Cell-penetrating peptides (CPPs) are cationic peptides that are able to induce cellular uptake and delivery of large and hydrophilic molecules, that otherwise do not cross the plasma membrane of eukaryotic cells. Despite their potential use for gene transfer and drug delivery, the mode of action of CPPs is still mysterious. Nonetheless, the interaction with phospholipid bilayers constitutes the first step in the process. The interaction of two CPPs with distinct charge distribution, penetratin (nonamphipathic) and RL16 (a secondary amphipathic peptide with antimicrobial properties) with lipid membranes was investigated. For this purpose, we employed three independent techniques, comprising ^{31}P-nuclear magnetic resonance, differential scanning calorimetry (DSC), and plasmon waveguide resonance (PWR) spectroscopy. In view of the cationic nature of the peptides, their interaction and affinity for zwitterionic *versus* anionic lipids was investigated. Although a strong affinity was observed when negative charged lipids were present, the peptides' thermodynamic behavior on binding to zwitterionic *versus* anionic lipids and the induced supramolecular structure organization in those lipids was quite different. The study suggests that the amphipathic profile and charge distribution of CPPs strongly influences the perturbation mechanism of the peptide on the bilayer establishing the frontier between a pure CPP and a CPP with antimicrobial properties.

Keywords: cell-penetrating peptide; antimicrobial peptide; peptide-membrane interaction; lipid supramolecular organization; differential scanning calorimetry; plasmon waveguide resonance spectroscopy; ^{31}P-NMR

Introduction

The cellular delivery of large and hydrophilic therapeutics needs to overcome the difficult transportation through the cell membrane. To help with overcoming this barrier, several classes of cell-penetrating peptides (CPPs) have been proposed during the last decade [1–3]. Despite their potential role in therapeutic target delivery in the cell, their uptake mechanism is far from being completely understood and has been at the center of debate since their discovery. Although different uptake mechanisms have been proposed to explain the entrance of such molecules inside the cell, either involving accessory proteins (endocytic pathways) or not, the first stage in the process consists of the interaction of those molecules with the cell membrane and so with the lipid molecules in the bilayer. In view of the high degree of complexity of cell membranes involving a great variety of proteins and lipid molecules to which carbohydrates add to the level of complexity, we have used lipid model systems to study their interaction mechanism and peptide effect on the lipid reorganization.

In the present study, we investigate in detail the interactions of two cationic CPPs, possessing distinct charge distribution, with several bilayer models: penetratin, one of the most well-known CPPs, that corresponds to the third helix of the Antennapedia homeodomain [4,5] (H-RQIKIWFQNRRMKWKK-NH_2); and RL16, an amphipathic peptide designed from structure–uptake relationships of penetratin [6] (H-RRLRRLLRRLLRRLRR-NH_2). Both peptides have been proposed as vectors to address biological molecules [7]. The large charge at physiological pH of those peptides excludes the passive diffusion across the lipid bilayer. Regarding penetratin, classical uptake mechanisms such as protein-based receptors and transporters appear not to be involved [5] as its uptake was not inhibited at 4 °C (energy independent), and it was found to be highly efficient and noncell-type specific. Moreover, penetratin is not sufficiently hydrophobic to insert deeply into the phospholipid model membranes [8]. Several mechanisms have been proposed for its uptake, such as the transient formation of inverted

* *Correspondence to: Isabel D. Alves, UPMC, UMR 7613, case courier 182, 4 place Jussieu, 75005 Paris, France. E-mail: isabel.alves@upmc.fr*

a *UPMC Univ Paris 06, UMR 7613 Synthèse, Structure et Fonction de Molécules Bioactives, FR 2769, Paris, France*

b *CNRS, UMR 7613, Paris, France*

c *UPMC, Proteomics and Mass Spectrometry Platform, IFR83, Paris, France*

d *Department of Biochemistry and Molecular Biophysics, University of Arizona, Tucson, AZ, USA*

‡ *11th Naples Workshop on Bioactive Peptides.*

micelles [6,9], electroporation-like permeabilization mechanisms [10,] and endocytosis [11–13]. It is also becoming clear that the internalization mechanism may depend on the chemical nature of the peptide and that some CPPs may use more than a single mechanism of internalization. Regarding RL16, this peptide permeabilizes eukaryotic cells, induces calcein leakage from large unilamellar vesicles (LUVs) [14] and was recently shown to have antimicrobial properties [15].

Herein, with the aim of contributing to the mechanistic understanding of the peptide/lipid interactions as a step toward their uptake mechanism, a combination of three biophysical techniques was employed using lipid model systems: ^{31}P-nuclear magnetic resonance (NMR), differential scanning calorimetry (DSC), and plasmon waveguide resonance (PWR) spectroscopy. As for the lipid model systems, we have used multilamellar vesicles (MLVs) for the DSC and NMR studies and a single solid-supported lipid bilayer with a plateau Gibbs border for the PWR studies. The use of distinct model systems, imposed by each technique itself can be advantageous as properties such as membrane curvature will be distinct for each model system, allowing one to look at this effect on the peptide/lipid interaction. At the same time, the differences between the different models used need to be kept in mind in the analysis of the results. In order to investigate the role of electrostatic interactions, the binding of the peptides with zwitterionic dimyristoyl phosphatidylcholine (DMPC) and anionic dimyristoyl phosphatidylglycerol (DMPG) lipids was investigated. With DSC, the effect of the peptide on the thermodynamics and cooperativity of the lipid phase transition and pre-transition was followed. The degree of perturbation in the energetic parameters of pre-transition and main phase transitions provides a good idea about the level of the insertion of the peptide in the lipid bilayer. The affinity of the peptides to solid-supported lipid bilayers composed of egg phosphatidylcholine (PC), and egg PC and palmitoyl phosphatidylglycerol (POPG) (3 : 1 mol/mol) were monitored directly (without the use of any labels) and in real time with PWR, by following the changes in the optical properties of the proteolipid system. In addition, due to the use of both *p*- and *s*-polarized light to produce resonance, this technique provides not only affinity constants (like any other surface plasmon resonance technique), but also permits a distinction between changes in mass and anisotropy of anisotropic and molecular-oriented systems, such as the case of a solid-supported lipid bilayer, used in those studies [16–18]. The peptide effect on the supramolecular organization of the lipids was investigated by ^{31}P-NMR, using DMPC and DMPG MLVs, which were studied at temperatures below, at, and above the phase transition temperature of the lipids. This technique has been widely used to follow the formation of different lipid phases such as hexagonal, cubic, and isotropic phases. The information obtained sheds some light on the mechanism of action of those peptides and the role of peptide charge distribution in the balance between cell-penetrating and antimicrobial properties of CPPs.

Materials and Methods

Materials

DMPC and DMPG were purchased from Genzyme (Switzerland) and were used without further purification. Egg PC and POPG were purchased from Avanti Lipids (AL, USA).

Peptide Synthesis

Peptides were assembled by stepwise solid-phase synthesis on an ABI 433A peptide synthesizer (Applied Biosystems) using standard Boc strategy (MBHA-PS resin with a loading of 0.9 mmol NH_2/g, amino acid activation with DCC/HOBt or HBTU) on a 0.1 mmol scale. The peptides were cleaved from the resin by treatment with anhydrous HF (1 h 30 min, 0 °C) in the presence of anisole (1.5 ml/g peptidyl-resin) and dimethylsulfide (0.25 ml/g peptidyl-resin) following the standard procedure. They were purified by preparative reverse-phase HPLC on a C8 column, using a linear acetonitrile gradient in an aqueous solution containing 0.1% (v/v) trifluoroacetic acid. Peptides were obtained with a purity >95%, as assessed by analytical HPLC. They were characterized by MALDI-TOF MS (Voyager Elite, PerSeptive Biosystems) in positive ion reflector mode using the matrix CHCA.

Preparation of MLVs

Lipid films were made by dissolving the appropriate amounts of lipid in a mixture of chloroform and methanol, 2/1 (v/v), followed by solvent evaporation under nitrogen to deposit the lipid as a film on the wall of a test tube. Final traces of solvent were removed in a vacuum chamber attached to a liquid nitrogen trap for 3–4 h. Films were hydrated with 10 mM Tris, 0.1 M NaCl, 2 mM EDTA, pH 7.6 (Tris buffer) and vortexed extensively at a temperature above the phase transition temperature of the lipid to obtain MLVs. The peptide was either codissolved with the lipid (for ^{31}P-NMR studies) or added after the formation of the MLVs (DSC studies).

Differential Scanning Calorimetry

The calorimetry was performed on a high-sensitivity differential scanning calorimeter (Calorimetry Sciences Corporation). A scan rate of 1 °C/min was used and there was a delay of 10 min between sequential scans in a series that allows for thermal equilibration. Data analysis was performed with the fitting program CPCALC provided by CSC and plotted with Igor. The total lipid concentrations used were 1 mg/ml, considering full hydration of the phospholipid mixtures. As for the peptide, P/L molar ratios of 1/100, 1/50, 1/25, and 1/10 were used in those studies. Samples containing the peptide alone dissolved in buffer at peptide concentrations corresponding to those at the higher peptide/lipid molar ratios studied (P/L 1 : 10); they exhibited no thermal events over the temperature range of 0–100 °C. This indicates that the peptides do not denature over this temperature range and that the endothermic events observed in this study do not arise from peptide unfolding but mainly from lipid phase transitions and lipid/peptide interactions. A minimum of at least three to four heating and cooling scans were performed for each analysis depending on whether or not the spectra were reproducible.

^{31}P-Nuclear Magnetic Resonance Spectroscopy

Multilamellar lipid samples were prepared using 10 mg of lipid, as described previously, in Tris buffer containing 10% D_2O. The peptide was either codissolved with the lipid before MLV formation or added after liposome formation at a P/L molar ratio of 1/25. The addition of the peptide after MLV formation is preferred as it better mimics the biological system, but in the case of DMPG MLVs strong precipitation of the sample was observed when the peptide was added to the lipid after MLV formation; we were hence obligated to do otherwise. The NMR spectra were collected

at several temperatures: below, at, and above the phase transition temperature of the lipid. The ^{31}P-NMR spectra were acquired on a Bruker DRX-500 spectrometer operating at 202.36 MHz for ^{31}P equipped with a 10-mm multinuclear probe and a Silicon Graphics workstation. Chemical shifts were determined relative to external 85% H_3PO_4. Before FT, a 30-Hz exponential line broadening was applied to the FID. The samples for NMR were prepared from 10 mg of lipid dispersed in 2.6 ml of H_2O. FIDs were acquired over 24.3 kHz with 32 K data points and 26 000 scans. A pulse width of 12 µs (~60° rotation angle), a relaxation delay of 2 s, and full-power proton decoupling with an RF field of 3125 Hz was employed. The temperature was controlled by using a Bruker variable-temperature unit.

Plasmon Waveguide Resonance Spectroscopy

PWR spectra are produced by resonance excitation of conduction electron oscillations (plasmons) by light from a polarized CW laser (He–Ne; wavelength of 632.8 and 543.5 nm) incident on the back surface of a thin metal film (Ag) deposited on a glass prism and coated with a layer of SiO_2 (see Ref. 16 for additional information). Experiments were performed on a beta PWR instrument from Proterion Corp. (Piscataway, NJ) that had a spectral resolution of 1 mdeg. The sample to be analyzed (a lipid bilayer membrane) was immobilized on the resonator surface and placed in contact with an aqueous medium, into which peptides can be introduced. The self-assembled lipid bilayers were formed using a solution (in butanol/squalene 0.93/0.07 v/v) of 8 mg/ml of lipid (either egg PC or a 3/1 mol/mol mixture of egg PC and POPG). The method used to make the lipid bilayers is based on the procedure by Mueller and Rudin to make black lipid membranes across a small hole in a teflon block [18]. To accomplish this, a small amount of lipid solution was injected into the orifice in a teflon block separating the silica surface of the PWR resonator from the aqueous phase. Spontaneous bilayer formation was initiated when the sample compartment was filled with aqueous buffer solution (see Ref. 16). The molecules (such as lipids and peptides) deposited onto the surface plasmon resonator change the resonance characteristics of the plasmon formation and can thereby be detected and characterized. PWR spectra, corresponding to plots of reflected light intensity *versus* incident angle, can be excited with light whose electric vector is either parallel (s-polarization) or perpendicular (p-polarization) to the plane of the resonator surface. Spectral simulation [16] and/or graphical analysis [19] allow one to obtain information about changes in the mass density, structural asymmetry, and molecular orientation induced by bimolecular interactions occurring at the resonator surface. Here, the graphical analysis method was employed. Briefly, this method consists of deconvoluting the components of the PWR spectra that are caused by changes in mass in the lipid film from those that are caused by changes in structural anisotropy. Such distinction can be done based on the magnitude and direction of the PWR spectra shifts observed for the *p*- and *s*-polarized light. Thus, alterations in mass density (due to addition or subtraction of mass from the membrane) result in shifts in p- and s-polarization with the same magnitude and direction (isotropic changes), whereas structure alterations lead to anisotropic changes (shifts for p- and s-pol that are distinct in magnitude and direction). By plotting the spectral changes observed in a (s, p) coordinate system where mass (Δ_m) and anisotropy (Δ_{str}) axes are represented based on the PWR sensitivity factor, the contribution of mass and structural changes can be obtained [19]. Each point in the mass and anisotropy axis can be expressed by changes in the original coordinates (Δp and Δs) by the following equations:

$$\Delta_m = [(\Delta s)^2{}_m + (\Delta p)^2{}_m]^{1/2} \quad (1)$$

$$\Delta_{str} = [(\Delta s)^2{}_{str} + (\Delta p)^2{}_{str}]^{1/2} \quad (2)$$

The sensitivity factor (S_f), a measure of the sensitivity of the instrument for the s-pol relative to p-pol ($S_f = \Delta s/\Delta p$), necessary to determine the mass and anisotropy axes has been determined, for the prism used in those experiments, to be 0.74 [20].

Affinities between the peptide and the lipids were obtained by plotting the PWR spectral changes that occur upon incremental additions of ligand to the cell. As the PWR is mainly sensitive to the optical properties of material that is deposited on the resonator surface [when a similar emergent medium (buffer) is employed, which is the case here], there is little interference from the material that is in the bulk solution. Moreover, the amount of bound material is much smaller than the total amount of ligand present in the bulk solution, and it is assumed that the bulk material is able to freely diffuse and equilibrate with the membrane. Data fitting (GraphPad Prism) through a hyperbolic saturation curve provides the dissociation constants. It should be noted that as concomitantly with the binding process other processes, such as membrane reorganization and solvation occur, the dissociation constants correspond to apparent dissociation constants.

Results

Peptide Effect on the Lipid Supramolecular Organization Investigated by ^{31}P NMR

^{31}P NMR was employed to assess the effect of the peptides on the lipid supramolecular structure organization. To understand the role of electrostatic interactions on the peptide-induced lipid organization, the NMR spectral lines of DMPC and DMPG MLVs were monitored in the absence or presence of RL16 and penetratin. The NMR signal was acquired at several temperatures: below, at, and above the phase transition temperature of the lipid.

The addition of RL16 to DMPC MLVs leads to the appearance of an isotropic signal at 0 ppm, which is characteristic of isotropic lipid assemblies such as micelles, or cubic phases in rapid diffusion (Figure 1). The isotropic linewidth at half-height ($\Delta\nu_{1/2}$) was determined to be between 170 and 420 Hz and to decrease with increase in the temperature, except at 32 °C, where a mixture of isotropic lines and powder pattern is observed. Such $\Delta\nu_{1/2}$ correspond to small structure assemblages such as small unilamellar vesicles, discs, or large micelles or bicelles. The coexistence of an isotropic line with a powder pattern at 32 °C disappeared when the temperature was raised to 50 °C (data not shown). The addition of the peptide to MLVs greatly reduced the turbidity of the liposome solution both below and above the phase transition temperature but increased it around the lipid phase transition temperature, concomitant with the appearance of lamellar phases. As for penetratin, its addition did not change the DMPC NMR spectral lines, hence lamellar structures were observed without fragmentation or micellization.

Regarding DMPG, a powder pattern, typical of lamellar phases, was observed below, at, and above the phase transition temperature, which above the phase transition coexisted with a small signal below 0 ppm that has been attributed to the formation of hexagonal phases (H_{II}) [21,22] (Figure 2). The presence of RL16 leads to the disappearance of such signal indicating

Journal of PeptideScience

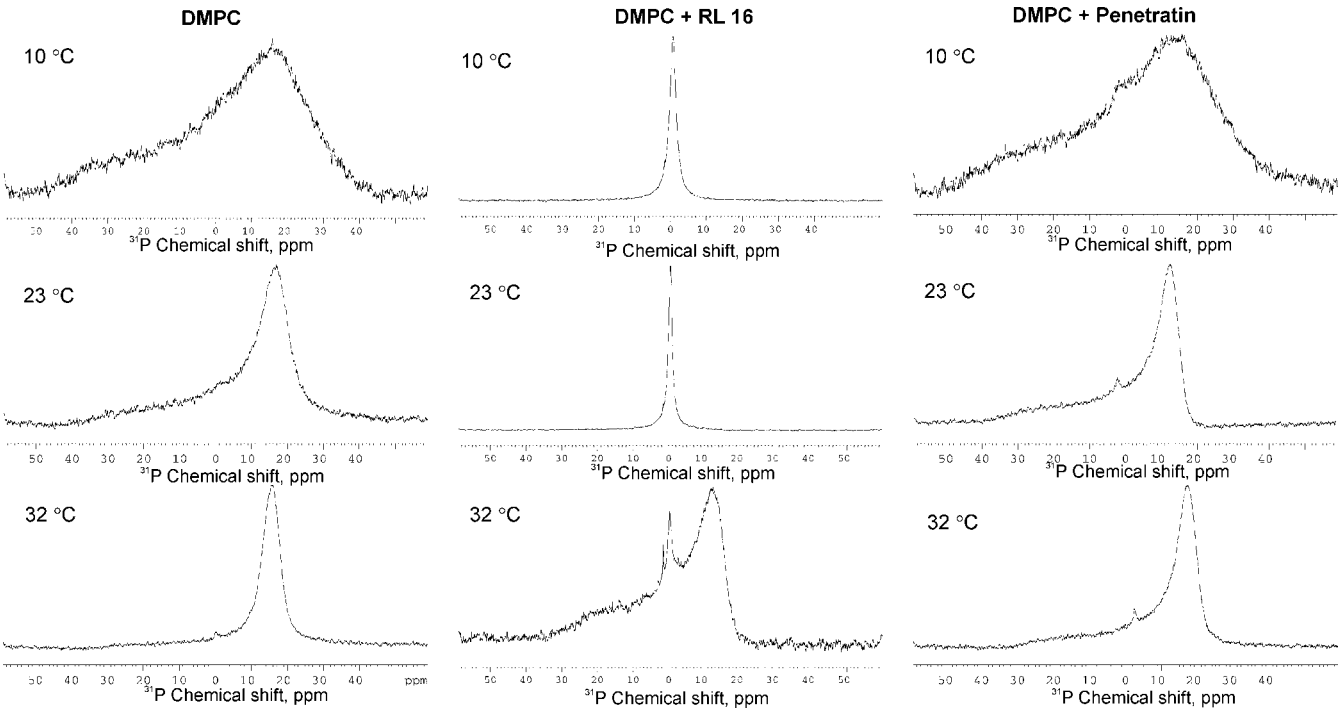

Figure 1. ^{31}P NMR spectra of DMPC multilamellar vesicles (first column) in the presence of RL16 (middle column) and penetratin (right column) at a P/L of 1/25 in the gel phase (10 °C), at approximately T_m (23 °C), and in the fluid phase (32 °C). The $\Delta\nu_{1/2}$ observed was 420, 250, and 535 Hz for the temperatures of 10, 23, and 32 °C, respectively. It should be noted that the DMPC/RL16 mixture when exposed to 50 °C resulted in an isotropic signal similar to that observed at 10 and 23 °C but with a smaller $\Delta\nu_{1/2}$ of 180 Hz.

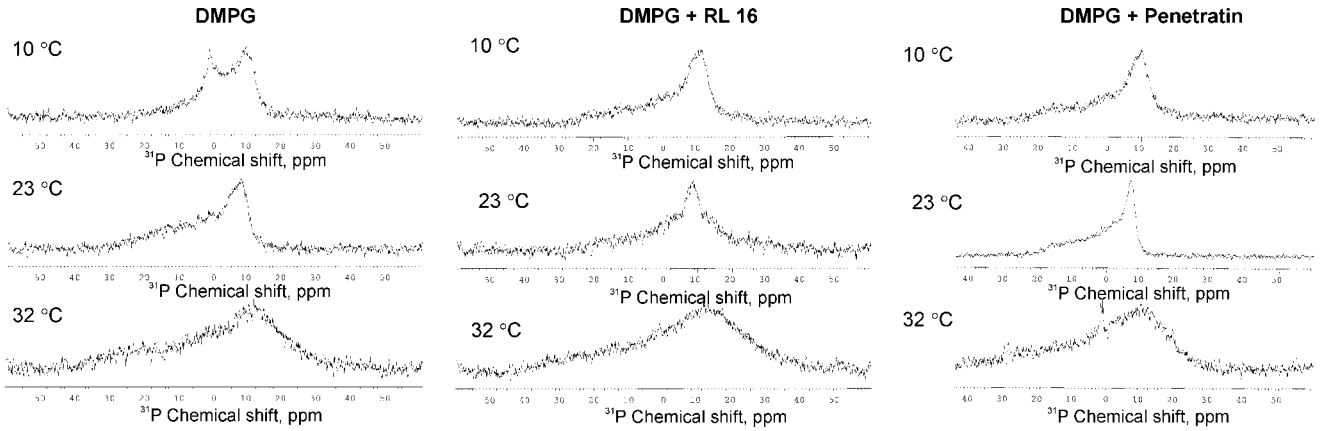

Figure 2. ^{31}P NMR spectra of DMPG multilamellar vesicles (first column) in the presence of RL16 (middle column) and penetratin (right column) at a P/L of 1/25 in the gel phase (10 °C), at approximately T_m (23 °C), and in the fluid phase (32 °C).

that the peptide disfavors a negative curvature in the bilayer. Such results correlate well with the tendency of this peptide to form lamellar phases as determined by the increase in the lamellar (L_α) to hexagonal (H_{II}) phase temperature transition (T_H) of Dipalmitoleoylphosphatidylethanolamine (DiPoPE) studied by DSC [15]. Concerning penetratin, the addition of the peptide after MLV formation produced a powder pattern below, at, and above the phase transition temperature with the presence of a signal below 0 ppm observed below the phase transition temperature. This indicates that penetratin may induce H_{II} phase formation. Again, such results are in agreement with DSC experiments showing that this peptide decreases the lamellar (L_α) to hexagonal (H_{II}) phase transition (T_H) of DiPoPE and so induces negative curvature formation [15].

Peptide Effect on Lipid Phase Transition Monitored by Calorimetry (DSC)

The degree of interaction of the peptide with lipids was monitored by following the changes in lipid phase pre-transition arising from the conversion of $L_{\beta'}$ to $P_{\beta'}$, and the main phase transition corresponding to the conversion from $P_{\beta'}$ to L_α (T_m) upon peptide/lipid interaction. In those studies the peptide was added to the lipid after MLV formation to better mimic the biological system. Many calorimetric studies have reported a codissolution of the peptide with the lipid prior to lipid film hydration and vesicle formation, especially in peptides that are not water soluble. As our peptides are water soluble we have not performed the experiments in this way. Such studies have been performed with a P/L molar

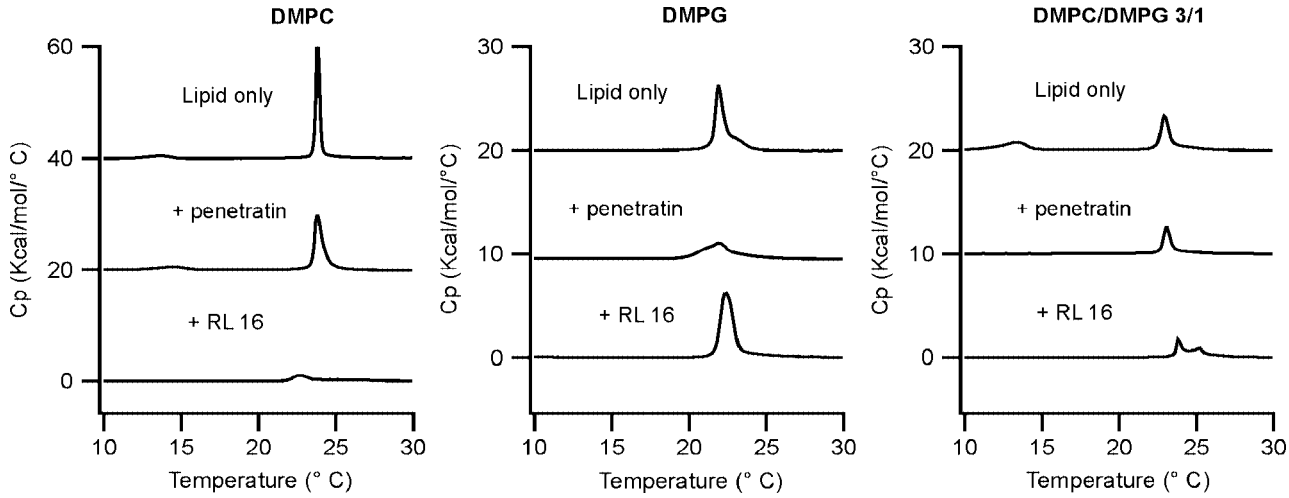

Figure 3. High-sensitivity DSC heating scans illustrating the effect of the addition of RL16 and penetratin on the thermotropic phase behavior of DMPC, DMPG, and DMPC/DMPG (3/1 mol/mol) multilamellar vesicles at a P/L 1/25. Thermodynamic parameters are given in Table 1.

Table 1. Thermodynamic parameters obtained by DSC for the interaction of penetratin and RL16 with MLVs of DMPC, DMPG, and DMPC/DMPG (3/1 mol/mol)

Lipid	P	T_m (°C)	ΔH_m (kcal/mol)	T_{pre} (°C)	ΔH_{pre} (kcal/mol)
DMPC	0	23.8	6.6	13.6	0.9
	Penetratin	23.8	7.1	14.5	1.2
	RL16	22.6/~26	2.4	–	–
DMPG	0	22.1	6.2	8.6	0.4
	Penetratin	21.9	3.8	–	–
	RL16	22.4	6.2	–	–
DMPC/DMPG 3/1 mol/mol	0	22.8	5.6	9.7	0.5
	Penetratin	22.9	4.7	–	–
	RL16	23.8	2.6	–	–

ratio of 1/100, 1/50, 1/25, and 1/10, although we just show here the P/L 1/25 results. It should be noticed that such P/L ratios result in peptide concentrations that are in tens to hundreds of micromolar, which correlate well with the antimicrobial activities of such peptides [15]. Moreover, uptake of penetratin in Chinese hamster ovarian (CHO) cells has been observed using about 10–20 μM [23,24]. The interaction of RL16 with DMPC MLVs clearly affects the thermotropic lipid behavior with abolishment of the pre-transition (at P/L ratio $\geq$ 1/25 and dramatic reduction at P/L of 1/100 and 1/50) and great reduction in the main phase transition temperature (T_m), the cooperativity and the enthalpy (Figure 3 and Table 1 for thermodynamic parameters). The enthalpy of the main phase transition is mainly due to the disruption of van der Waals interactions between the fatty acid chains, and perturbations on this transition are indicative of intercalation of the peptide between the fatty acid chains. This indicates a strong interaction of RL16 with this lipid, not only at the level of the headgroup but also with an intercalation in between the fatty acid chains; this will be further discussed in the following section. As for penetratin, no major effects were observed in the main phase transition: no change in the phase transition temperature, small change in enthalpy, and a small decrease in the cooperativity of the transition. The results indicate that penetratin interacts weakly with this lipid.

In the case of DMPG, the main transition is not symmetric and exhibits a marked high-temperature shoulder, which is due to the low ionic strength used in this experiment [25]. This temperature shoulder becomes less pronounced in the presence of RL16 due to the electrostatics interaction of the peptide with the lipid surface, which reduces the charge–charge repulsion of the lipid headgroups. In contrast to what was observed in the case of DMPC, RL16 has a minor effect on the phase transition of DMPG. The perturbation of RL16 on the pre-transition of the lipid (which is abolished at a P/L of 1/50) and very small effect on the energetic of the main transition indicates that the peptide interacts mainly at the headgroup level without deeply inserting in the hydrophobic core. The preferential interaction of the peptide with anionic lipids is explained by the presence of ten positive charges in the peptide. The negative charges in the membrane surface immobilize the peptide and prevent its insertion in the core region. Contrary to what was observed with RL16, penetratin has a strong effect on both the pre-transition and the main phase transition. The pre-transition, which is observed in some saturated lipids, is due to the tilting of the hydrocarbon side chains and is quite sensitive to the presence of the interacting molecules. The untilting of the hydrocarbon chains by penetratin may be explained by a simple neutralization of the headgroup charge by the cationic peptide, which will result in reduced electrostatic headgroup repulsion and

concomitantly in a smaller headgroup area observed in the case of DMPG. Regarding the main phase transition, a 60% decrease in enthalpy was induced by penetratin, indicating some level of peptide insertion within the acyl chain region.

As for the interaction of the peptides with a 3/1 mol/mol mixture of DMPC/DMPG, both penetratin and RL16 lead to the disappearance of the pre-transition and to a decrease in the enthalpy of the main phase transition, which were more pronounced in the case of RL16. These results correlate well with the observation that this peptide had a stronger effect on the lipid phase transition of DMPC, the major lipid in the present mixture.

A splitting in the thermogram has been observed both for RL16 and penetratin that we attribute to inhomogeneous distribution of the peptide in the lipid leading to the formation of peptide-poor (corresponding to the sharper transition where the lipid transition is less perturbed) and peptide-enriched (corresponding to the broad and less cooperative transition where the lipid transition is more perturbed) areas. Such behavior has been observed by other laboratories for the interaction of antimicrobial peptides with membranes [26–29].

Peptide Interaction with Planar Lipid Bilayers Monitored by PWR

This technique was used to directly monitor the interaction of penetratin and RL16 with the lipid bilayer and the peptide-induced changes in the lipid mass density and organization. One should point out that the lipid employed here was egg PC, with or without POPG, rather than DMPC and DMPG as used in the DSC and NMR studies, which are more biological-relevant lipid mixtures. Moreover, it is much easier to prepare solid-supported lipid bilayers composed of egg PC than a single lipid. Alternatively, doing DSC studies with egg PC would have resulted in complicated and rather energetically unfavorable transitions. PWR spectral changes occurring after the addition of penetratin to the PWR cell compartment containing an egg PC bilayer are shown in Figure 4. The binding of penetratin to the egg PC bilayer produced a biphasic event, with decreases in the resonance angle position both for p- and s-pol. at low concentrations (up to 1 μM), followed by positive shifts for both polarizations at higher concentrations (>1 μM). In order to characterize the mass and the structural changes that accompany the interaction of the peptide with the lipid bilayer, one has to either obtain the optical parameters from the PWR spectra by fitting procedures (see Ref. 16 for details) or to use a more simple method based on graphical analysis that allows one to distinguish between mass and anisotropy changes (fully described in Ref. 19). Herein, we have chosen to perform a graphical analysis, which, by plotting the data points on a (s, p) coordinate system containing both mass and structural axis placed according to the sensitivity factor of the PWR sensor (See section on Materials and Methods for details), allows the determination of the mass and structural anisotropy contributions to the process (Figure 5). Thus, the origin of the plot corresponds to the lipid bilayer in the absence of ligand and the data points shown correspond to the shifts induced by peptide binding to the bilayer (at saturating concentrations where the signal reaches a plateau). The high-affinity binding process of penetratin falls in the third quadrant (negative values for both p- and s-shift) for which the following values of mass and structural changes were obtained: $\Delta s_m = -7$ mdeg; $\Delta p_m = -9$ mdeg; $\Delta p_{str} = 0$ mdeg; $\Delta s_{str} = 0$ meaning that a pure mass effect is observed. The mass changes correspond to a decrease in the mass density in the lipid bilayer, which can only be explained by an efflux of lipid out of the bilayer and into the plateau Gibbs border. This may be a consequence of repulsion between the positive charges in penetratin and those

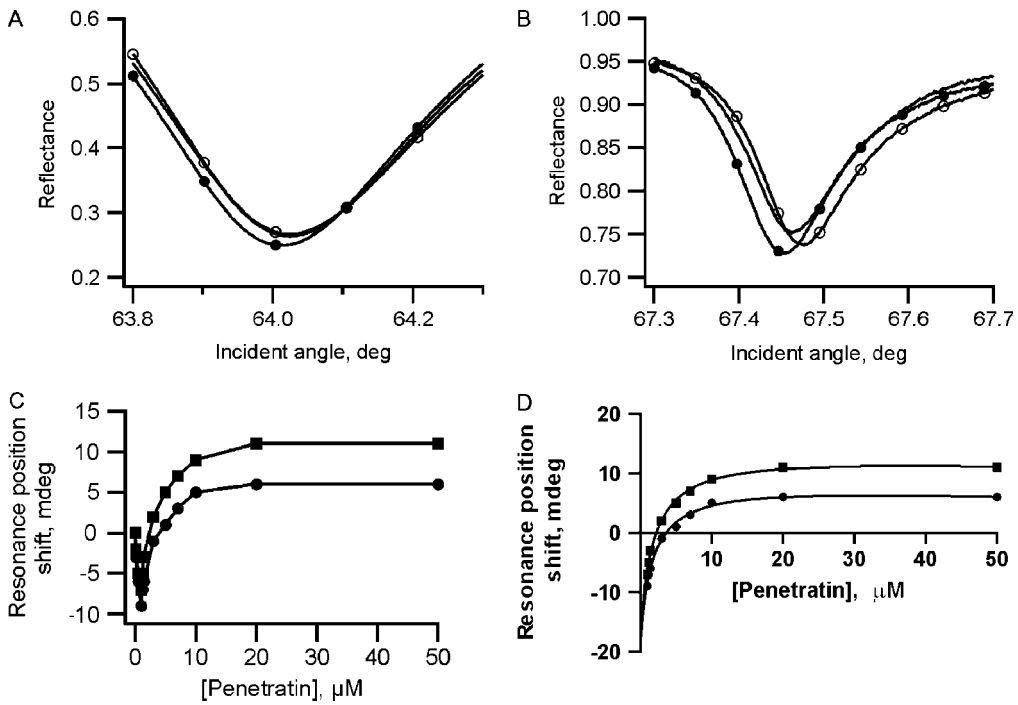

Figure 4. Interaction of penetratin with an egg PC lipid bilayer monitored by PWR. Panels A and B correspond to the PWR spectra obtained for the lipid bilayer (solid line) and after addition of about 1 μM (●) and of 50 μM (○) of penetratin to the bilayer obtained for *p*- and *s*-polarized light, respectively. The resonance position shifts obtained for p- (●) and s- (■) polarizations for the incremental addition of penetratin are represented (panel C) as well as the hyperbolic binding curve obtained for the low-affinity binding process (panel D).

in the phospholipid headgroups, as has been proposed earlier [30]. As for the second event, the low-affinity binding process is placed in the first quadrant in the coordinate system (Figure 5). The analysis of this data point indicates a gain in mass density ($\Delta s_m = 16$ mdeg; $\Delta p_m = 21$ mdeg; corresponds to ~80% change in mass) accompanied by a small change in the anisotropy of the system ($\Delta p_{str} = -6$ mdeg; $\Delta s_{str} = 2$ mdeg; corresponds to ~20% change in structure). Moreover, from this second event, an apparent dissociation constant ($K_{D\ app}$) of 1.8 μM was obtained for penetratin interaction (See section on Materials and Methods for the procedure). Such biphasic behavior was not observed for the interaction of penetratin with an egg PC/POPG (mol/mol) bilayer, where only positive shifts were observed [30]. A 20-fold increase in the binding affinity was observed for this lipid (data not shown), indicating that electrostatics plays a role in penetratin interaction with the bilayer. A comparison of the magnitude of the spectral shift observed with *p*- and *s*-polarized light in the weak binding event (Figure 4, panel C) indicates that the shifts obtained with *s*-polarized light are larger than those obtained with *p*-polarized light. As several studies have suggested that the peptide adopts a helical structure (anisotropic structure) in contact with lipids, such spectral changes may indicate that the peptide is placed with its long axis parallel to the lipid bilayer.

The addition of increasing amounts of RL16 to an egg PC bilayer produced a very different PWR response, as one can see in Figure 6, a monophasic response was observed with decreases in the resonance angle position both for *p*- and *s*-polarized light. The magnitude of the resonance angle shift was similar for both polarizations (see panel C) and was about 60 mdeg (approx. −61 mdeg for p-pol and approx. −58 mdeg for s-pol). This is a very large spectral shift, corresponding in magnitude to about 1/3 of that obtained upon the formation of the lipid bilayer (when compared to the buffer spectra). Such large spectral changes indicate that the peptide induces large structural and mass changes in the lipid bilayer. As can be seen in Figure 5, the binding of RL16 to the lipid bilayer falls in the third quadrant of the plot (corresponding to negative values for both p- and s-shifts) meaning that the ligand mainly induces decreases in the mass density of the lipid. From the positions of the mass and structure axis, one can calculate the coordinates of this point relative to the coordinate system, given by $\Delta p_m = -71$ mdeg; $\Delta s_m = -54$ mdeg; $\Delta p_{str} = 10$ mdeg; and $\Delta s_{str} = -4$ mdeg as shown in Figure 5. Using Eqns (1) and (2), the values of a pure mass effect and a pure structural effect were calculated, indicating that structural changes account for ~10% of the spectral changes,

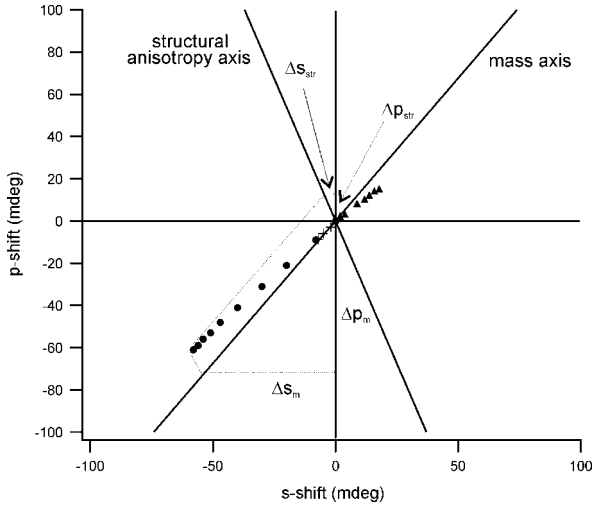

Figure 5. Plots of the PWR spectral shifts on a (s, p) coordinate system presenting the mass and structural anisotropy axes for the interaction of RL16 (●) and penetratin for both the high-affinity (+) and low-affinity (▲) processes. The s- and p-coordinates describing the mass (Δp_m and Δs_m) and structural shifts (Δp_{str} and Δs_{str}) for the interaction of RL16 with the lipid bilayer are presented (dotted lines), which have been calculated using Eqns (1) and (2) and a sensitivity factor ($S_f = \Delta s/\Delta p$) of 0.74.

whereas mass changes account for ~90%. A decrease in mass density in this case, where mass is being added by RL16 binding to the bilayer, results mainly from a decrease in the mass of the lipid bilayer due to removal of lipid from the bilayer accompanied by lipid structural rearrangements. As noted earlier, a similar behavior was observed in the case of the bilayer composed of egg PC and POPG (3 : 1 mol/mol). Regarding the affinity of RL16 to the bilayer, a subpicomolar affinity was observed for both lipid bilayer compositions. It should be noted that this represents an apparent dissociation constant reflecting both the interaction of the peptide with the bilayer and also the removal of lipid from the bilayer. We have tried to distinguish the two processes by performing kinetic experiments at distinct peptide concentrations. In those experiments, the resonance minimum of the spectra is followed as a function of time. A biphasic signal was observed in the first seconds, no change in the resonance minima was observed, probably corresponding to the phase where the peptide was binding, followed by a gradual decrease in the resonance angle position, which equilibrated after a few minutes (data not shown). The time length of the first process decreased with increases in

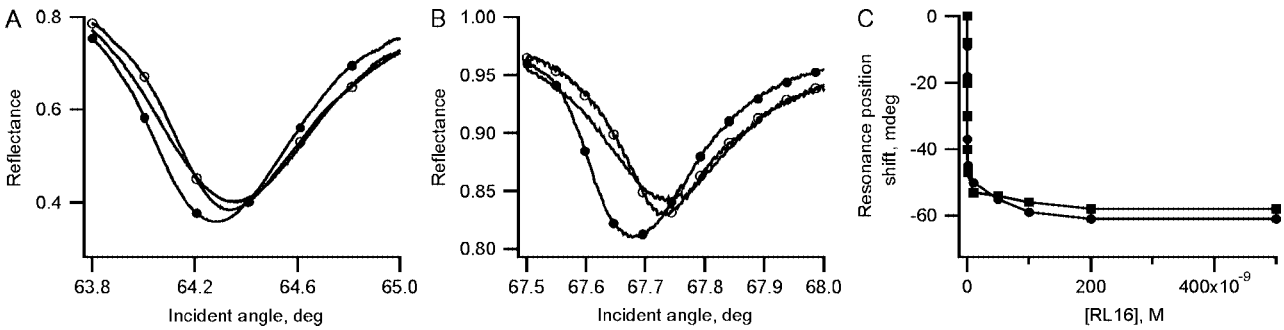

Figure 6. Interaction of RL16 with an egg PC lipid bilayer monitored by PWR. Panels A and B correspond to the PWR spectra obtained for the lipid bilayer (solid line) after addition of saturating concentrations of peptide (●) and after washing the PWR cell sample with buffer (○) obtained for *p*- and *s*-polarized light, respectively. The binding curve obtained for the interaction of RL16 with the bilayer obtained for p- (●) and s- (■) polarizations is presented in panel C.

Journal of PeptideScience

peptide concentration, making it difficult to distinguish the two processes. Experiments are under way to further investigate the kinetics of the process.

Discussion

Using a combination of biophysical techniques: ^{31}P-NMR, DSC, and PWR spectroscopy, the interaction of two cationic CPPs with lipid model systems was investigated. Important information regarding the affinity of those peptides for the lipid bilayer (zwitterionic and anionic), the degree of interaction, and the changes in the supramolecular organization of the lipid and mass density were obtained. A detailed characterization of the peptide–membrane interactions is essential to determine the molecular mechanisms responsible for the cell-penetrating activities of those peptides.

Penetratin, one of the most studied CPPs, is a cationic nonamphipathic peptide that is unstructured in solution and in the presence of uncharged lipid bilayers, but adopts a helical structure in the presence of negatively charged lipids [15,31,32]. The widespread interest that this peptide has attracted resides on its ability to directly target conjugated oligopeptides to the cytoplasm and nuclear compartments of cells [9]. Apart from the fact that this peptide does not perturb membrane integrity, which excludes a permeabilization of the membrane by pore formation, its uptake mechanism remains highly controversial up to now. Penetratin leads to a powder pattern in the ^{31}P-NMR spectra in DMPC MLVs and induces the formation of a nonlamellar structure in DMPG above the phase transition temperature. The induction of vesicle formation by penetratin has been reported recently in the case of egg PC bilayers [33]. A preferential and stronger interaction of penetratin for anionic *versus* zwitteronic lipids was observed in our studies. DSC shows that the peptide leads to a great perturbation of the thermodynamics of both the pre-transition and the main phase transition of DMPG, which indicates that the peptide interacts with this lipid at the headgroup level and has some degree of insertion in the acyl chain region. In the case of DMPC, no significant effect in the lipid phase transition was observed. Moreover, a slight decrease in T_m is observed, which correlates with a preferential interaction of the peptide with a fluid bilayer. PWR studies confirm the role of electrostatics in the penetratin/lipid interaction as a 20-fold increase in the affinity was observed in the presence of negatively charged lipids. The fact that an interaction was monitored by PWR between penetratin and egg PC but no perturbation in the phase transition of DMPC was observed by DSC may be explained by the great diversity in fatty acid chain composition in egg PC (also, residual amounts of other lipids than PC are possible). The complexity in the lipid composition of egg PC makes this lipid rather unfavorable for DSC studies. The greater magnitude in the s-pol shift *versus* p-pol by PWR studies indicates that the peptide may orient parallel to the lipid bilayer, and this correlates with previous studies [34]. The electrostatic interaction between the arginine residues in the peptide and the lipid headgroups may trigger peptide structural changes creating hydrophobic patches in the peptide, which may allow a partial insertion in the membrane core region. The formation of nonlamellar structures in the presence of certain lipids such as DMPG (our studies) and egg PC [33] may correspond to the formation of small vesicles that detach from the bilayer or to the formation of inverted micelles. DSC studies on the effect of penetratin on the lamellar (L_α) to hexagonal (H_{II}) phase transition temperature (T_H) indicate that the peptide favors a negative curvature in the lipid bilayer [15] and X-ray studies recently published support this idea [33]. Such studies support the hypothesis that penetratin may enter cells by the formation of inverted micelles, entrapping the peptide across the bilayer and releasing it inside the cell. The cellular uptake of penetratin by the formation of inverted micelles although postulated and evidenced by model studies [1,5,6,15,33] has not directly been observed in cells and continues to be debated. Such process may require specific lipids to occur; hence, specific lipid recruitment may trigger the process and this is the current subject of investigation in our laboratory.

RL16, a perfect amphipathic peptide, derived from sequence uptake relationships of penetratin, adopts an alpha helical structure both in solution and in the presence of lipids and has been determined to possess antimicrobial properties [15]. Their antimicrobial properties correlate with the fact that this peptide perturbs the cell membrane integrity [15] probably due to the formation of pores in the membrane. ^{31}P-NMR studies reported here show that the addition of RL16 to MLVs of DMPC leads to the formation of small objects, which according to the $\Delta\nu_{1/2}$ may correspond to discs or vesicles. At the phase transition temperature these objects coexist with lamellar phases. A similar behavior has been observed for the interaction of melittin with DPPC, where an isotropic signal was observed both below and above the phase transition temperature and a mixture of a powder pattern and an isotropic signal was observed around the phase transition temperature [35]. Membrane fragmentation has been observed for other antimicrobial peptides such as a magainin analog (MSI-78) [36], gramicidin [37] and also in the case of the CPPs TAT and Arg8 in the presence of DMPC but not in DMPG [38]. The fragmentation of the membrane by RL16 correlates well with the PWR studies that show that the peptide induces a decrease in mass in the proteolipid system. In order to confirm that the decrease in mass was due to lipid being removed from the lipid bilayer in the form of fragments and not due to lipid that moved into the plateau Gibbs border, the bulk solution in the PWR cell sample has been analyzed by MALDI-TOF MS confirming the presence of both the peptide and the lipids in the solution. In the case of penetratin, no lipids were found in the bulk solution of the cell. Moreover, the increase in the T_H of DiPoPE observed by DSC is also in favor of the induction of positive curvature in the lipids by this peptide [15], which exists in small structures such as vesicles or discs. The DSC studies indicate that RL16 has a strong perturbation in the lipid chain packing of DMPC, suggesting that the peptides insert deeply in the membrane. In the case of DMPG, the peptide rather stays at the lipid headgroup level, as only the pre-transition temperature is affected. Placing the results obtained in terms of an interaction mechanism, the peptide has a strong affinity for bilayers (both zwitterionic and anionic) to which it initially binds parallel to the membrane. In case of anionic bilayers, the peptide will interact with the bilayer through its hydrophilic side, which leads to peptide/peptide interaction to avoid exposure of the hydrophobic face of the peptide to water, and this is accompanied by aggregation of liposomes (data not shown). The peptide stays immobilized in the surface due to electrostatic interaction between the phospholipids groups and the arginines in the peptide that impedes the peptide to penetrate deep in the bilayer. In the case of zwitterionic bilayers, the hydrophobic interaction of the peptide with the lipid will prevail leading to an intercalation of the peptide in between

the fatty acid chains. An electrostatic repulsion between the exposed charged surfaces of peptides placed in adjacent bilayers is created, which leads to the disruption of MLVs. This process is accompanied by membrane fragmentation. The fragmentation of the lipid bilayer is a reversible process as peptide removal from the lipid (PWR experiments described earlier) leads to a recovery of the lipid bilayer. This result may explain the fact that this peptide is not toxic for eukaryotic cells at the concentrations at which it has antimicrobial activities without lysis in *S. staphylococcus aureus* (9 μM) [15]. We suggest that RL16 acts by a detergent-like carpet mechanism, the peptide first assembling in the membrane surface followed by a membrane permeation and disintegration by a detergent-like mechanism [39]. During this process the formation of transient pores may occur, as it has been suggested that the formation of 'holes' or toroidal pores may occur as an early step in the membrane fragmentation process. Pore formation without the complete progression to membrane disruption has been seen in many antimicrobial peptide (AMP) such as magainin.

As far as sequence/activity relationships of CPPs are concerned, they appear not to share common motifs apart from being rich in arginines and being internalized by a receptor-independent mechanism. Their basic character alone is not sufficient for the translocation as peptides rich in lysine get transducted with much less efficiency than arginine-rich peptides [38]. Other experiments agree with the idea that charge alone is not the only driving force, for example, the substitution in penetratin of two tryptophanes by phenylalanines strongly diminishes translocation [4]. Increasing the number of clustered positively charged amino acids enhances attachment of a peptide to a membrane but it prevents its transport to the nucleus [37]. In terms of arginine-rich peptides it seems that an arginine octamer presents the optimal length for efficient uptake. Polymers composed of other positively charged amino acids such as lysine and histidine are not transduced implicating a role of the guanidinium in peptide activity [40,41] suggesting that H-bonding may be involved.

In conclusion, the studies performed demonstrate that the spatial charge distribution in the peptide sequence and the balance between lipophilic and hydrophilic forces between the peptide and the lipid lead to distinct mechanisms of interaction and reorganization of the bilayer. Whether such different bilayer interaction and perturbation mechanisms induced by the peptide result in different uptake processes is still a matter for debate. In any case, the study shows that the borderline between CPP and AMP activity and the capacity of a peptide to switch between those is highly modulated by charge distribution and amphipathicity of the peptide.

Acknowledgements

This work was supported by the Association Nationale pour la Recherche (ANR-Prob DOM).

References

1. Derossi D, Chassaing G, Prochiantz A. Trojan peptides: the penetratin system for intracellular delivery. *Trends Cell Biol.* 1998; **8**: 84–87.
2. Lindgren M, Hällbrink M, Prochiantz A, Langel U. Cell-penetrating peptides. *Trends Pharmacol. Sci.* 2000; **21**: 99–103.
3. Snyder EL, Dowdy SF. Cell penetrating peptides in drug delivery. *Pharm. Res.* 2004; **21**: 389–393.
4. Derossi D, Joliot AH, Chassaing G, Prochiantz A. The third helix of the Antennapedia homeodomain translocates through biological membranes. *J. Biol. Chem.* 1994; **269**: 10444–10450.
5. Derossi D, Calvet S, Trembleau A, Brunissen A, Chassaing G, Prochiantz A. Cell internalization of the third helix of the Antennapedia homeodomain is receptor-independent. *J. Biol. Chem.* 1996; **271**: 18188–18193.
6. Derossi D, Chassaing G, Prochiantz A. Trojan peptides: the penetratin system for intracellular delivery. *Trends Cell Biol.* 1998; **8**: 84–87.
7. Chassaing G, Prochiantz A. Peptides usable as vectors for the intracellular addressing of bioactive molecules. PCT Int. Appl, WO 9712912 : 31; 1997.
8. Drin G, Déméné H, Temsamani J, Brasseur R. Translocation of the pAntp peptide and its amphipathic analogue AP-2AL. *Biochemistry* 2001; **40**: 1824–1834.
9. Prochiantz A. Getting hydrophilic compounds into cells: lessons from homeopeptides. *Curr. Opin. Neurobiol.* 1996; **6**: 629–634.
10. Binder H, Lindblom G. Charge-dependent translocation of the Trojan peptide penetratin across lipid membranes. *Biophys. J.* 2003; **85**: 982–995.
11. Conner SD, Schmid SL. Regulated portals of entry into the cell. *Nature* 2003; **422**: 37–44.
12. Drin G, Cottin S, Blanc E, Rees AR, Temsamani J. Studies on the internalization mechanism of cationic cell-penetrating peptides. *J. Biol. Chem.* 2003; **278**: 31192–311201.
13. Fischer R, Köhler K, Fotin-Mleczek M, Brock R. A stepwise dissection of the intracellular fate of cationic cell-penetrating peptides. *J. Biol. Chem.* 2004; **279**: 12625–12635.
14. Lamaziere A, Burlina F, Wolf C, Chassaing G, Trugnan G, Ayala-Sanmartin J. Non-metabolic membrane tabulation and permeability induced by bioactive peptides. *PLoS ONE* 2007; **2**: e201.
15. Alves ID, Goasdoué N, Correia I, Aubry S, Galanth C, Sagan S, Lavielle S, Chassaing G. Membrane interaction and perturbation mechanisms induced by two cationic cell penetrating peptides with distinct charge distribution. *Biochim. Biophys. Acta* 2008; **1780**: 948–959.
16. Salamon Z, Macleod HA, Tollin G. Coupled plasmon-waveguide resonators: a new spectroscopic tool for probing proteolipid film structure and properties. *Biophys. J.* 1997; **73**: 2791–2797.
17. Tollin G, Salamon Z, Hruby VJ. Techniques: plasmon-waveguide resonance (PWR) spectroscopy as a tool to study ligand-GPCR interactions. *Trends Pharmacol. Sci.* 2003; **24**: 655–659.
18. Mueller P, Rudin DO, Tien HT, Wescott WC. Reconstitution of cell membrane structure in vitro and its transformation into an excitable system. *Nature* 1962; **194**: 979–980.
19. Salamon Z, Tollin G. Graphical analysis of mass and anisotropy changes observed by plasmon-waveguide resonance spectroscopy can provide useful insights into membrane protein function. *Biophys. J.* 2004; **86**: 2508–2516.
20. Devanathan S, Salamon Z, Tollin G, Fitch J, Meyer TE, Cusanovich MA. Binding of oxidized and reduced cytochrome c2 to photosynthetic reaction centers: plasmon-waveguide resonance spectroscopy. *Biochemistry* 2004; **43**: 16405–16415.
21. Verkleij AJ, de Kruijff B, Ververgaert PHJT, Tocanne JF, Van Deenen LLM. The influence of pH, Ca^{2+} and protein on the thermotropic behavior of the negatively charged phospholipids, phosphatidylglycerol. *Biochim. Biophys. Acta* 1974; **339**: 432–437.
22. Girault L, Boudou A, Dufourc EJ. 113Cd-, 31P-NMR and fluorescence polarization studies of cadmium (II) interactions with phospholipids in model membranes. *Biochim. Biophys. Acta* 1998; **1414**: 140–154.
23. Aussedat B, Sagan S, Chassaing G, Bolbach G, Burlina F. Quantification of the efficiency of cargo delivery by peptidic and pseudopeptidic Trojan carriers using MALDI-TOF mass spectrometry. *Biochim. Biophys. Acta* 2006; **1758**: 375–383.
24. Delaroche D, Aussedat B, Aubry S, Chassaing G, Burlina F, Clodic G, Bolbach G, Lavielle S, Sagan S. Tracking a new cell-penetrating (W/R) nonapeptide, through an enzyme-stable mass spectrometry reporter tag. *Anal. Chem.* 2007; **79**: 1932–1938.
25. Andrushchenko VV, Vogel HJ, Prenner EJ. Interactions of tryptophan-rich cathelicidin antimicrobial peptides with model membranes studied by differential scanning calorimetry. *Biochim. Biophys. Acta* 2007; **1768**: 2447–2458.
26. Henzler-Wildman KA, Martinez GV, Brown MF, Ramamoorthy A. Perturbation of the hydrophobic core of lipid bilayers by the human antimicrobial peptide LL-37. *Biochemistry* 2004; **43**(26): 8459–8469.
27. Prenner EJ, Lewis RN, Kondejewski LH, Hodges RS, McElhaney RN. Differential scanning calorimetric study of the effect of the antimicrobial peptide gramicidin S on the thermotropic phase

behavior of phosphatidylcholine, phosphatidylethanolamine and phosphatidylglycerol lipid bilayer membranes. *Biochim. Biophys. Acta* 1999; **1417**: 211–223.
28. Matsuzaki K, Sugishita K, Ishibe N, Ueha M, Nakata S, Miyajima K, Epand RM. Relationship of membrane curvature to the formation of pores by magainin 2. *Biochemistry* 1998; **37**: 11856–11863.
29. Adão R, Seixas R, Gomes P, Pessoa JC, Bastos M. Membrane structure and interactions of a short Lycotoxin I analogue. *J. Pept. Sci.* 2008; **14**: 528–534.
30. Salamon Z, Lindblom G, Tollin G. Plasmon-waveguide resonance and impedance spectroscopy studies of the interaction between penetratin and supported lipid bilayer membranes. *Biophys. J.* 2003; **84**: 1796–1807.
31. Magzoub M, Kilk K, Eriksson LE, Langel U, Gräslund A. Interaction and structure induction of cell-penetrating peptides in the presence of phospholipid vesicles. *Biochim. Biophys. Acta* 2001; **1512**: 77–89.
32. Christiaens B, Symoens S, Verheyden S, Engelborghs Y, Joliot A, Prochiantz A, Vandekerckhove J, Rosseneu M, Vanloo B. Tryptophan fluorescence study of the interaction of penetratin peptides with model membranes. *Eur. J. Biochem.* 2002; **269**: 2918–2926.
33. Lamazière A, Wolf C, Lambert O, Chassaing G, Trugnan G, Ayala-Sanmartin J. The homeodomain derived peptide Penetratin induces curvature of fluid membrane domains. *PLoS ONE* 2008; **3**: e1938.
34. Pott T, Paternostre M, Dufourc EJ. A comparative study of the action of melittin on sphingomyelin and phosphatidylcholine bilayers. *Eur. Biophys. J.* 1998; **27**: 237–245.
35. Hallock KJ, Lee D-K, Ramamoorthy A. MSI-78, an analogue of the magainin antimicrobial peptides, disrupts lipid bilayer structure via positive curvature strain. *Biophys. J.* 2003; **84**: 3052–3060.
36. Prenner EJ, Ruthven RNAH, McElhaney RE. The interaction of the antimicrobial peptide gramicidin S with lipid bilayer model and biological membranes. *Biochim. Biophys. Acta* 1999; **1462**: 201–221.
37. Afonin S, Frey A, Bayerl S, Fischer D, Wadhwani P, Weinkauf S, Ulrich AS. The cell-penetrating peptide TAT(48-60) induces a non-lamellar phase in DMPC membranes. *ChemPhysChem* 2006; **13**: 2134–2142.
38. Shai Y. Mode of action of membrane active antimicrobial peptides. *Biopolymers* 2002; **66**: 236–248.
39. Futaki S, Suzuki T, Ohashi W, Yagami T, Tanaka S, Ueda K, Sugiura Y. Arginine-rich peptides. An abundant source of membrane-permeable peptides having potential as carriers for intracellular protein delivery. *J. Biol. Chem.* 2001; **276**: 5836–5840.
40. Mitchell DJ, Kim DT, Steinman L, Fathman CG, Rothbard JB. Polyarginine enters cells more efficiently than other polycationic homopolymers. *J. Pept. Res.* 2000; **56**: 318–325.
41. Persson D, Thorén PE, Nordén B. Penetratin-induced aggregation and subsequent dissociation of negatively charged phospholipid vesicles. *FEBS Lett.* 2001; **505**: 307–312.

